Quantum Monte Carlo study of a vortex in superfluid ^{4}He and search for a vortex state in the solid

D. E. Galli,[1] L. Reatto,[2] and M. Rossi[3]

[1]*Dipartimento di Fisica, Università degli Studi di Milano, via Celoria 16, 20133 Milano, Italy*

[2]*via Bazzini 20, 20133 Milano, Italy*

[3]*Dipartimento di Fisica e Astronomia "Galileo Galilei", Università degli Studi di Padova, via Marzolo 8, 35131 Padova, Italy*

(Received 24 February 2014; revised manuscript received 25 April 2014; published 27 June 2014)

We have performed a microscopic study of a straight quantized vortex line in three dimensions in condensed ^{4}He at zero temperature using the shadow path integral ground state method and the fixed phase approximation. We have characterized the energy and the local density profile around the vortex axis in superfluid ^{4}He at several densities, ranging from below the equilibrium density up to the overpressurized regime. For the Onsager-Feynman (OF) phase our results are exact and represent a benchmark for other theories. The inclusion of backflow correlations in the phase improves the description of the vortex with respect to the OF phase by a large reduction of the core energy of the topological excitation. At all densities the phase with backflow induces a partial filling of the vortex core and this filling slightly increases with density. The core size slightly decreases for increasing density and the density profile has well defined density dependent oscillations whose wave vector is closer to the wave vector of the main peak in the static density response function rather than to the roton wave vector. Our results can be applied to vortex rings of large radius R and we find good agreement with the experimental value of the energy as a function of R without any free parameter. We have studied also ^{4}He above the melting density in the solid phase using the same functional form for the phase as in the liquid. We found that off-diagonal properties of the solid are not qualitatively affected by the velocity field induced by the vortex phase, both with and without backflow correlations. Therefore we find evidence that a perfect ^{4}He crystal is not a marginally stable quantum solid in which rotation would be able to induce off-diagonal long-range coherence.

DOI: 10.1103/PhysRevB.89.224516 PACS number(s): 67.25.dk, 03.75.Lm, 02.70.Ss, 05.30.−d

I. INTRODUCTION

Topological excitations represent a class of excitations of fundamental interest in many ordered phases in condensed matter such as Bose/BCS-condensed quantum fluids, superconductors, crystals, or nematic liquid crystals. Starting from the works by Onsager [1] and Feynman [2], a widely studied example of a topological excitation is a vortex line in a Bose superfluid, in particular in superfluid ^{4}He. Vortices play a fundamental role in many superfluid phenomena, for instance the behavior of a superfluid under rotation or the value of the critical velocity for the onset of dissipation in many cases are determined by vortex nucleation. Addressing specifically superfluid ^{4}He almost all the studies of vortices are based on simplified models in which vorticity turns out to be localized along mathematical lines, more precisely the phase of the wave function (wf) is assumed to be additive in the phase of each particle, the so called Onsager-Feynman (OF) form. Within this approximation the vorticity field has a singularity along a line, the vortex core, where the density vanishes and the velocity diverges. This behavior is found, for instance, with the Gross-Pitaevskii (GP) equation [3,4] or with the Biot-Savart model of vortex filaments [5]. Such models can be a reasonable approximation for weakly interacting particles such as cold bosonic atoms. For a strongly correlated system such as superfluid ^{4}He, that approximation is questionable because single particle phase additivity is incompatible with the presence of interparticle correlations that lead to backflow effects. Still, also in superfluid ^{4}He, most of the studies are based on models with singular vorticity. A justification for this is that the healing length ξ of the superfluid order parameter is of order 1 Å, orders of magnitude smaller than the typical intervortex distance. Therefore in most instances the flow field of a given vortex system is equal to that given by classical incompressible hydrodynamics with the single constraint that the circulation κ around each vortex filament is quantized in unit of Planck's constant over particle mass, $\kappa = h/m$. This explains why only few studies have addressed the local structure of a vortex in superfluid ^{4}He beyond the singular vorticity models.

The previous perspective is changing due to the intense experimental and theoretical interest in vorticity phenomena at low temperature [6,7], where the normal component of the superfluid essentially vanishes. Under such conditions diffusion and decay of a vortex tangle, as observed experimentally [8], must be dominated by reconnection of vortices, the only mechanism that can change the topology of the vortex system in the absence of dissipation. Computations [9] based on the GP equation show that reconnections take place when the distance between two vortex cores is of order the healing length ξ. On the basis of the GP equation the local density vanishes at the vortex line and the density reaches smoothly the bulk value within a distance of order ξ, whereas it is known that interparticle correlations lead to density oscillations as a function of distance from the vortex axis [10]. It should be noted that when the GP equation is used to study the elementary excitations of the system, the bulk excitations consist of phonons joining monotonically free particle behavior at large wave vectors and that roton excitations are not present. Rotons are excitations arising in the presence of strong interparticle correlations [11–14]. The nature of the bulk excitations can be relevant in connection with vortex reconnections because there is evidence that a reconnection event is associated with emission of bulk excitations, in addition to vortex oscillations

(Kelvin waves) [15]. More precisely studies based on the GP equation [16,17] have shown that vortex reconnection events generate rarefaction waves, i.e., bulk sound waves. This suggests that a realistic study of reconnections in superfluid ^{4}He needs to start from a good model of the vortex core and, at the same time, of the excitations of bulk superfluid ^{4}He with a proper treatment not only of phonons but also of rotons [18], the more so because on the basis of density functional theory it has been shown [19,20] that the oscillation of the density profile around the vortex core seems to be related to the roton excitations. Recent progress [21–23] in the visualization at a local level of quantum vorticity should allow studies of vortex reconnections and quantum turbulence at a level of detail not available before so that advances in theoretical modeling are called for.

In the literature only very few studies are present of the core of a vortex in superfluid ^{4}He based on microscopic theory that goes beyond the mean field singular vortex behavior. In three dimensional (3D) ^{4}He the only study is the one [24,25] based on variational theory with shadow wave function (SWF). Another study was presented of a vortex in superfluid ^{4}He in mathematical two dimensions (2D) based on the so called fixed phase quantum Monte Carlo (FP-QMC) [26]. Also FP-QMC is a variational approach but it goes beyond the approach of Refs. [24,25] because, for an assumed form of the phase of the wf, the real part of the wf is computed exactly. In these works [24–26] the global vortex phase is not additive in the single particle phases but it contains also pair or more complex contributions. Commonly one says that backflow effects are taken into account. This term has its origin in the Feynman-Cohen theory [11] of rotons in which the phase of such momentum carrying excited state has not only single particle contributions, like in the Feynman theory [27], but also contributions depending on the relative positions of pairs of neighboring atoms. Such pair contributions are needed in order to guarantee local conservation of matter and there is some similarity with the backflow effects in classical hydrodynamics. A visualization of such roton backflow can be found in Ref. [12] where roton wave packets have been studied by a microscopic theory. As far as we know, no study of a vortex in the 3D ^{4}He based on advanced QMC methods has been performed yet and this is the problem that we address in the present study of a straight vortex line in condensed ^{4}He via the shadow path integral ground state [28,29] (SPIGS) method with fixed phase approximation. We have studied a vortex line in superfluid ^{4}He over an extended pressure range, from a density below equilibrium close to the spinodal up to a density in the deeply overpressurized liquid ^{4}He at a density about 15% above the freezing density.

Following our recent work on 2D *solid* ^{4}He [30], here we have studied also a possible vortex state in 3D solid ^{4}He by considering different phases with FP-QMC. This investigation is motivated by the presence of phenomenological models based on vortices [31] to explain the possible superfluid response of solid ^{4}He [32], i.e., supersolidity. In fact, the vortex model has been used to interpret several experiments [33–36]. Supersolidity in solid ^{4}He is a debated question [32] and there is no shared consensus on the supersolid nature of ^{4}He. A point that is firmly established by QMC computations is that in an ideal perfect (i.e., with no defects, the so called commensurate crystal) ^{4}He crystal the condensate fraction and the superfluid density are zero at finite [37,38] and even at zero temperature [39,40]. In the absence of phase coherence our choices for the phase of the wave function [Eqs. (3) and (6)] have little justification. The conjecture has been put forward that the nonsupersolid state of ^{4}He could be marginally stable (i.e., almost any deviation from the perfect crystal would lead to a superfluid response) [32,40]. Then, the present computation is relevant to infer whether the centrifugal barrier associated with the flow field of a vortex line is able to induce in an ideal perfect crystal off-diagonal long-range order.

This paper is organized as follows: In Sec. II we discuss the fixed phase approximation applied to the simulation of a vortex line with the path integral ground state method; our results for a straight vortex line in the liquid phase of ^{4}He are shown in Sec. III and how our results can be applied to a vortex ring of large diameter is discussed in Sec. IV. In Sec. V we present the results for the solid phase and Sec. VI contains our conclusions.

II. METHODS

Dealing with vortices in a Bose fluid is an unresolved problem for exact microscopic *ab initio* methods, and it calls for some approximations or assumptions. For instance, in order to describe a straight vortex line, the many-body wf $\Psi(R)$ has to be an eigenstate of the angular momentum operator $\hat{\mathcal{L}}_z$ with eigenvalues $\hbar N l$, $l = 1,2,\ldots$ being the quanta of circulation; this requires the presence of a phase and thus one deals with a complex wave function. It seems really tempting, following the well established route for the ground state, to try improving a variational ansatz by exploiting the projection ability of exact quantum Monte Carlo (QMC) techniques. Unfortunately the complex nature of the wf rules out an exact implementation of QMC methods due to the presence of a phase problem. The most followed recipe is then to overcome the sign problem by releasing the exactness of QMC techniques and improving only some aspects of the trial wf, keeping other aspects at a variational level. This is the case of approximations such as fixed phase [26,41] or fixed node [42]. Such approximations are viable also with finite temperature methods that do not involve explicitly the wf, such as path integral Monte Carlo [43].

In full generality, the many-body wf can be written as $\Psi(R) = e^{i\Omega(R)}\Psi_0(R)$, where $\Omega(R)$ is the phase and $\Psi_0(R)$ is the modulus of the wf, and $R = \{\vec{r}_1,\vec{r}_2,\ldots,\vec{r}_N\}$ represents the coordinates of the N particles composing the system. $\Psi(R)$ describes a stationary quantum state if it is a solution of the time independent Schrödinger equation $\hat{\mathcal{H}}\Psi(R) = E\Psi(R)$, from which two coupled differential equations for $\Omega(R)$ and $\Psi_0(R)$ are readily obtained. The fixed phase approximation [26] consists in assuming a given functional form for the phase $\Omega(R)$ and in solving the remaining differential equation for the modulus $\Psi_0(R)$:

$$\left[-\frac{\hbar^2}{2m}\sum_{i=1}^{N}\nabla_i^2 + V_\Omega(R) + V(R)\right]\Psi_0(R) = E_\Omega\Psi_0(R), \quad (1)$$

where $V(R)$ represents the interatomic potential of the system and $V_\Omega(R)$ reads

$$V_\Omega(R) = \frac{\hbar^2}{2m}\sum_{i=1}^{N}(\vec{\nabla}_i\Omega(R))^2\,. \tag{2}$$

Solving Eq. (1) is equivalent to solving the original time independent Schrödinger equation for the N particles with the extra potential term $V_\Omega(R)$. Equation (1) can now be solved with one of the QMC methods that give the exact energy and other properties of the system. It can be proved that the fixed phase method provides a variational upper bound for the lowest energy state among the wave functions having the assumed phase $\Omega(R)$ [26].

In the case of a straight vortex line, the simplest possible choice for the phase is the well known Onsager-Feynman (OF) phase [2]:

$$\Omega^{\rm OF}(R) = \sum_{i=1}^{N}\theta_i, \tag{3}$$

where θ_i is the azimuthal coordinate of the ith particle with respect to the vortex axis. $\Omega^{\rm OF}(R)$ gives rise to an irrotational flow field everywhere but on the vortex axis where the velocity field diverges and the quantized vorticity is localized on this axis. The extra potential term $V_\Omega(R)$ in Eq. (1) is given by the standard centrifugal barrier:

$$V_\Omega^{\rm OF}(R) = \sum_{i=1}^{N} v_\Omega^{\rm OF}(r_i) \tag{4}$$

with

$$v_\Omega^{\rm OF}(r_i) = \frac{\hbar^2}{2m}\frac{1}{r_i^2}, \tag{5}$$

where r_i is the radial cylindrical coordinate of the ith particle. Due to the divergence of $V_\Omega^{\rm OF}(R)$ when a particle approaches the vortex axis, the local density has to vanish on the vortex line in order to have finite kinetic energy. The OF recipe, which provides a vortex line with a hollow core and localized vorticity, has been largely employed to predict the properties of a vortex line in the ground state of bulk ^{4}He via integral equation [10], density functional [19], and variational Monte Carlo (VMC) [25,44] methods, and some of these techniques have been applied with good results also to Bose-condensed gases [45].

A way to improve the OF ansatz is taking into account the so called backflow (BF) correlations [26] such that $V_\Omega(R)$ is no longer a sum of single particle terms and, by a proper choice of the phase, the velocity field can remain finite everywhere, also at the vortex core, and the vorticity is no longer localized. With the choice of Ref. [26] for the phase, it is found that BF correlations lower the vortex energy compared to the OF choice (that computation covers only 2D ^{4}He [26,42]) and, more important, it has a dramatic effect on another property of the system: the vortex core turns out to be no longer empty [26,46] but the density is finite even inside the core. Similar results in 3D have been also reached with the SWF variational technique: the lowest energy state has a partially filled core with distributed vorticity over a radius of about 1 Å [25,44,47].

In the present computation we assume for $\Omega(R)$ of a straight vortex line a form that is an extension in 3D of the form studied by Ortiz and Ceperley in Ref. [26] in 2D. Our BF phase $\Omega^{\rm BF}(R)$ reads

$$\Omega^{\rm BF}(R) = \sum_{j=1}^{N}\ln\left(\frac{A_j + iB_j}{\sqrt{A_j^2+B_j^2}}\right) \tag{6}$$

with $A_j = x_j + k\sum_{l\neq j} f(|\vec{r}_{jl}|,r_j,r_l)(x_j - x_l)$ and $B_j = y_j + k\sum_{l\neq j} f(|\vec{r}_{jl}|,r_j,r_l)(y_j - y_l)$. $f(|\vec{r}_{jl}|,r_j,r_l) = \exp-[\alpha|\vec{r}_{jl}|^2 + \gamma(r_j^2+r_l^2)]$ is the BF function [26] characterized by the variational parameters k, α, and γ, and $|\vec{r}_{jl}| = |\vec{r}_j - \vec{r}_l|$. In Eq. (6) we have used Cartesian coordinates with the z axis taken along the vortex axis and $r_j = \sqrt{x_j^2+y_j^2}$. The wf $\Psi(R)$ constructed with $\Omega^{\rm BF}(R)$ has some analogy with the Feynman-Cohen wf for the phonon-roton excited states [11]. With this choice of the phase, the extra potential term in Eq. (1) reads

$$V_\Omega^{\rm BF}(R) = \sum_{i=1}^{N} v_{\Omega i}^{\rm BF}(R) \tag{7}$$

with

$$v_{\Omega i}^{\rm BF}(R) = \frac{\hbar^2}{2m}\left(\frac{A_i\nabla_i B_i - B_i\nabla_i A_i}{A_i^2+B_i^2} + \sum_{l\neq i}\frac{A_l\nabla_i B_l - B_l\nabla_i A_l}{A_l^2+B_l^2}\right)^2. \tag{8}$$

For comparison purpose we have also performed computations for zero backflow (i.e., for $k = 0$) so that one recovers the OF phase (3).

We face the task of solving (1) with the extra potential $V_\Omega^{\rm OF}(R)$ and $V_\Omega^{\rm BF}(R)$ with the shadow path integral ground state (SPIGS) method [28,29], which allows us to obtain the exact lowest eigenstate of a given Hamiltonian and the exact correlation functions by projecting in imaginary time τ with the operator $e^{-\tau\hat{H}}$ a SWF [48] taken as a trial wf. As SWF we have used the optimized form [49] for bulk ^{4}He. It has been verified [50] that the SPIGS method is unbiased by the choice of the trial wf, but a good choice of the trial wf is important in order to accelerate convergence as a function of imaginary time and to reduce fluctuations. Therefore in a SPIGS computation the only inputs are the interparticle potential and the approximation for the imaginary time propagator [50]. By a proper choice of the propagator the resulting errors can be reduced below the statistical uncertainty of the computation. Notice that as trial wf we have used a wf for the bulk system which is uniform. The nonuniformity induced by the vortex phase is exclusively due to the action of the imaginary time evolution operator $e^{-\tau\hat{H}}$, so that by construction no bias is introduced in the computation once the phase factor has been chosen. This is a great advantage of a SPIGS computation compared, for instance, to the case of a computation with the Green's function and diffusion MC as in Refs. [26,42].

As He-He interatomic potential we have considered the HFDHE2 Aziz potential [51] and for the imaginary time propagator we have employed the primitive approximation.

The chosen time step is $\delta\tau = 1/640$ K^{-1} and the total projection time is $\tau = 0.5$ K^{-1}, which represent a good compromise between accuracy and computational cost.

A technical difficulty with both (4) and (7) is represented by their long-range character which complicates the use of a finite simulation cell with periodic boundary conditions (pbc). Often this problem has been overcome by simulating the system in a finite bucket [25,26], but this has the drawback that two inhomogeneities are present at the same time, the one due to the vortex and the one due to the confining well. Another possibility is to study a vortex-antivortex lattice in the bulk system so that no large scale flow field is present and one can use pbc [44]. This approach brings in computational complications and it is difficult to implement with our form of BF. On the other hand the vortex-antivortex lattice computation has shown that BF modifies the velocity flow field from the one of OF only at very short distance from the core, below about 1 Å. Since we are interested in the characterization of local properties around the vortex core we have adopted a shortcut: we have simply smoothed the extra potentials $V_\Omega^{\rm OF}$ and $V_\Omega^{\rm BF}$ far from the core multiplying the terms $v_\Omega^{\rm OF}$ and $v_{\Omega i}^{\rm BF}$ in (4) and (7) by the following function:

$$\mathcal{S}(r) = \begin{cases} 1, & r < \Delta, \\ e^{-(r-\Delta)^2/(r-L/2)^2}, & \Delta \leqslant r \leqslant L/2, \\ 0, & r > L/2 \end{cases} \qquad (9)$$

(L being the side of the simulation box), so that standard pbc can be applied. With this choice, the extra potential is equivalent to (4) and (7) for $r < \Delta$, and gently smoothed to zero by $\mathcal{S}(r)$ in the range $\Delta \leqslant r \leqslant L/2$. The provided $\Psi(R)$ is no longer an exact eigenstate of $\hat{\mathcal{L}}_z$ but we have verified that the local quantities we want to characterize, such as the integrated energy around the vortex line and the density around the core, are not affected by the value of Δ, once it is taken sensibly greater than the core width. The results shown in the next sections correspond to the choice $\Delta = 8$ Å.

III. VORTEX LINE IN SUPERFLUID ^{4}He

We have studied a straight vortex line in bulk superfluid ^{4}He at $T = 0$ K at four different densities: near equilibrium density, $\rho = 0.0218$ Å^{-3}, near the freezing density, $\rho = 0.026$ Å^{-3} ($P = 25$ bars), below the equilibrium density, $\rho = 0.02$ Å^{-3} ($P = -6$ bars), and finally, well above the freezing density, for a metastable overpressurized liquid, $\rho = 0.03$ Å^{-3} ($P = 71$ bars). The reported values of pressure are derived from the theoretical equation of state [52] for the adopted He-He interatomic potential. The initial particle configurations for the metastable disordered computation have been obtained by rescaling to the desired density configurations from a simulation performed below freezing; in this way, as shown in Ref. [52], even at $\rho = 0.03$ Å^{-3} the system remains disordered allowing for the characterization of the properties of the overpressurized phase. The number of particles in the simulation box was taken to be $N = 336$, which is large enough to ensure negligible size effects. The adopted BF phase function, Eq. (6), has three backflow parameters, the amplitude k, the interparticle range α, and the particle-vortex range γ, and these have been determined by minimization of the total energy of the vortex. Computations at $\rho = 0.0218$ Å^{-3} have given $\alpha = 0.1377$ Å^{-2} and $\gamma = 0.0765$ Å^{-2} (which correspond to a length scale of about 1.9 and 2.5 Å, respectively); these optimal values of α and γ turn out to be equal to those obtained for the 2D system [26]. Therefore we have retained these values also for all the other densities considered here. Given this value for γ, we expect that the effect of the backflow will be restricted mainly within about 2.5 Å from the vortex line. The optimization of the backflow parameter k gave the following optimal values: $k = 0.8$ at $\rho = 0.02$ Å^{-3}, $k = 0.7$ at $\rho = 0.0218$ Å^{-3}, $k = 0.6$ at $\rho = 0.026$ Å^{-3}, and $k = 0.6$ at $\rho = 0.03$ Å^{-3}. When $k = 0$ no vortex backflow effect is present and one recovers the OF phase Eq. (3) which has no variational parameters.

In Fig. 1 we show the integrated vortex energy per unit length $\varepsilon_v(r) = [E_v(r) - E(r)]/L_z$ as a function of radial distance r for the BF and OF phase. L_z is the box side along the vortex axis and $E_v(r)$ and $E(r)$ are, respectively, the energy of the particles that lie inside the cylinder of radius r centered on the z axis in the system with and without the vortex line. Therefore $\varepsilon_v(r)$ represents the vortex excitation energy per unit length integrated up to the radial distance r. We plot $\varepsilon_v(r)$ up to a distance of 8 Å because beyond this distance the vortex flow field is modified with respect to the hydrodynamic $1/r$ as discussed in the previous section, so that $\varepsilon_v(r)$ for $r > 8$ Å does not have physical meaning. It is evident from Fig. 1 that at all densities the BF phase (6) reduces sensibly the energy of the vortex line excitation with respect to the OF phase; as expected, backflow mostly affects the integrated vortex energy within about 2 Å. Beyond this distance the two phases are essentially the same and we found that the energy gap $\Delta\varepsilon_v(r) = \varepsilon_v^{\rm BF}(r) - \varepsilon_v^{\rm OF}(r)$ for $r > 2$ Å is almost constant within the statistical uncertainties. The average of $\Delta\varepsilon_v(r)$ over the range $2 < r < 3$ Å is $\overline{\Delta\varepsilon_v} = -0.62 \pm 0.02$ K at $\rho = 0.02$ Å^{-3}, -0.59 ± 0.01 K at $\rho = 0.0218$ Å^{-3}, -0.93 ± 0.01 K at $\rho = 0.026$ Å^{-3}, and -1.00 ± 0.01 K at $\rho = 0.03$ Å^{-3}. If we take $\varepsilon_v(r)$ at $r = 2$ Å as a measure of the vortex core energy it turns out that the core energy given by BF is less than half that of the OF phase. More precisely, the ratio $\eta = \varepsilon_v^{\rm BF}(r)/\varepsilon_v^{\rm OF}(r)$ at $r = 2$ Å takes the values $\eta = 0.35$, 0.52, 0.37, and 0.30 at the four densities of our computations, going from the lowest to the highest.

Classically, the vortex energy in an incompressible fluid has a logarithmic dependence on r. For a vortex line with circulation κ this classical energy per unit length is usually written as

$$\varepsilon_{\rm hyd}(r) = \frac{\kappa^2}{4\pi} m\rho \left[\ln \frac{r}{a} + \delta \right], \qquad (10)$$

where a is assumed as a core parameter and δ is related to the model for the core [5,53]. For instance, one has $\delta = 0$ for a hollow core model and $\delta = 1/4$ for a core of radius a rotating at uniform angular velocity as a solid body (solid core model) [53,54]. The specific model chosen for the vortex core is a matter of taste unless one wishes to obtain absolute data [55] and one goes outside the hydrodynamics of an incompressible fluid. The parameters a and δ are clearly not

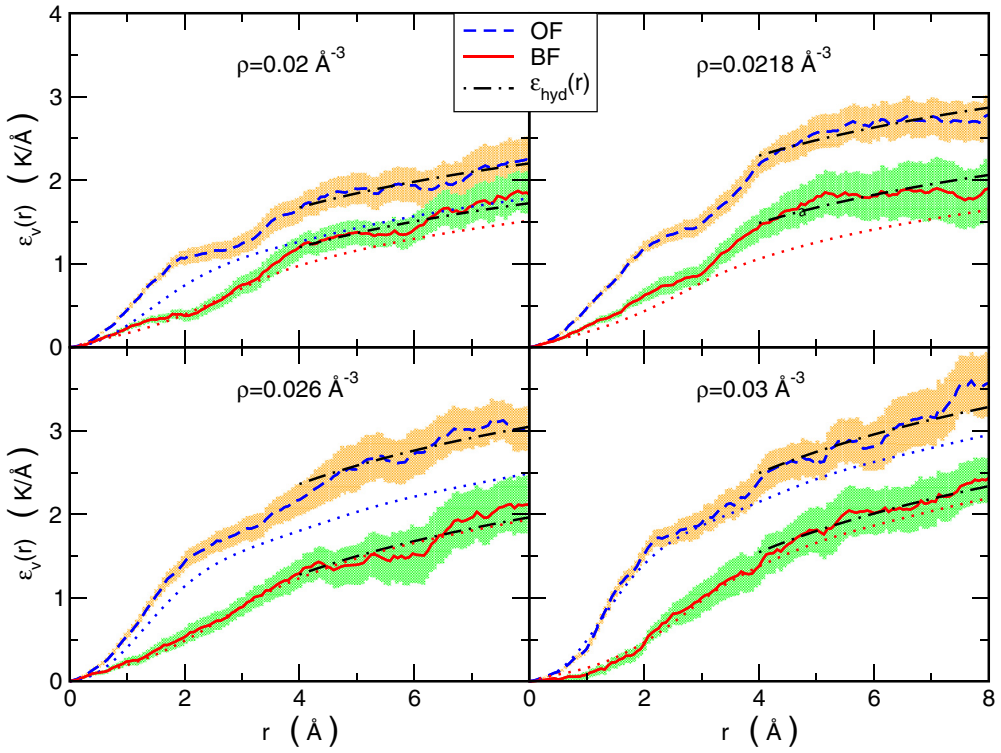

FIG. 1. (Color online) Integrated energy up to a distance r of a straight vortex line per unit length, $\varepsilon_v(r)$, at different densities in the liquid phase as a function r. Dashed line: Onsager-Feynman phase. Solid line: Backflow phase. The shadings represent the statistical uncertainties of the results. Dotted lines: Integrated phase kinetic energy per unit length $v(r) = V_\Omega(r)/L_z$, where $V_\Omega(r)$ is the extra potential energy due to the vortex phase of the particles that lie in the cylinder of radius r. Dot-dashed line: Fit of the MC data with the hydrodynamic form Eq. (11).

independent and Eq. (10) can be written in the form

$$\varepsilon_{\rm hyd}(r) = \frac{\hbar^2}{m}\pi\rho \ln\frac{r}{\lambda}, \tag{11}$$

where the core parameter lambda is $\lambda = ae^{-\delta}$ and the quantum value $\kappa = h/m$ for the circulation has been used. For a quantum vortex within the GP equation the energy can be written in the form (11) only for r large compared to the coherence length as discussed below.

Our results for the quantum vortex give $\varepsilon_v(r)$ that is a slowly increasing function of r with some structure that can be connected to the oscillations of the density profile as discussed below. However, statistical uncertainties are too large to characterize in detail such structures. Our results for the energy of the quantum vortex for r not too small can be represented in a reasonable way by the functional form (11) for a suitable choice of λ. A fit of $\varepsilon_v(r)$ with $\varepsilon_{\rm hyd}(r)$ over the range 4–8 Å gives the values of λ reported in Table I and the corresponding $\varepsilon_{\rm hyd}(r)$ is plotted in Fig. 1 as a dot-dashed line. For a vortex in bulk ^{4}He at distances larger than 8 Å the contribution to the vortex energy due to interparticle correlations and to backflow should have decayed to zero and the density is uniform so that the only remaining contribution to $\varepsilon_v(r)$ is the kinetic energy due to the $1/r^2$ centrifugal barrier. Therefore Eq. (11) is the correct representation of the vortex energy also at arbitrary large distance for a straight vortex in bulk ^{4}He. It should be stressed again that the parameter λ for the quantum vortex is just a convenient way to represent the energy of the quantum vortex such that it joins with the large scale behavior and λ does not represent the core radius or the healing length. In summary, both for the OF and the BF phase Eq. (11) is a good representation of the quantum $\varepsilon_v(r)$ starting from $r > 4$ Å; below this distance $\varepsilon_{\rm hyd}(r)$ does not represent the quantum energy and one should use the numerical results reported in Fig. 1.

The vortex excitation energy $\varepsilon_v(r)$ can be decomposed into several contributions. One derives from the expectation value of the extra potential $V_\Omega(R)$ and this corresponds to the kinetic energy due to the phase of the wave function.

TABLE I. Parameter λ from the fit of the quantum vortex energy per unit length with the hydrodynamic Eq. (11) in the region 4–8 Å, and values of the parameter Λ, Eq. (18), for the energy of a large vortex ring obtained from the present calculations (SPIGS) compared to the values obtained with SWF [25] (SWF) and with the values obtained by fitting the experimental data [55] (exp.).

			Λ (Å)		
ρ (Å^{-3})	phase	λ (Å)	SPIGS	SWF	exp.
0.020	OF	0.45(2)	3.32(4)		
	BF	0.85(2)	6.03(8)		
0.0218	OF	0.25(1)	1.87(2)	2.72	5.98
	BF	0.67(2)	5.1(1)	5.87	
0.026	OF	0.38(1)	2.72(3)		7.68
	BF	1.13(3)	8.2(1)		
0.030	OF	0.46(2)	3.27(4)		
	BF	1.05(2)	7.62(5)		

TABLE II. Core radii $d_{\rm WHM}$ and $R_{\rm cyl}$ as defined in the text at different densities for both OF and BF phases. Integrated energy per unit length of a vortex line at 6 Å from the core for the present computations (SPIGS) and for the variational approach of Ref. [25] (SWF). Damping parameter r_1 in Eq. (14). Wave vector $q_{\rm max}$ of the first peak of $\tilde{\rho}(q)$, roton wave vector $q_{\rm rot}$ from Ref. [52], and position of the main peak, q_χ, in the static density response function, $\chi(q)$ [64], computed via the GIFT method [63]. q_χ has been obtained from a parabolic fit of $\chi(q)$ in the region of the main peak (data at 0.020 and 0.030 Å^{-3} are from unpublished computations).

		core radius		$\varepsilon_v(r=6$ Å$)$ (K/Å)					
ρ (Å^{-3})	phase	$d_{\rm WHM}$ (Å)	$R_{\rm cyl}$ (Å)	SPIGS	SWF	r_1 (Å)	$q_{\rm max}$ (Å^{-1})	$q_{\rm rot}$ (Å^{-1})	q_χ (Å^{-1})
0.020	OF	0.923	1.003	1.94(21)		2.48	1.91(2)	1.844(3)	1.936(2)
	BF	0.668	0.963	1.42(17)		3.13	1.91(2)		
0.0218	OF	0.885	0.928	2.67(21)	2.36	3.07	1.97(3)	1.908(6)	1.989(3)
	BF	0.663	0.753	1.81(29)	1.91	3.46	1.97(1)		
0.026	OF	0.821	0.606	2.74(27)	2.97	3.40	2.09(1)	2.048(6)	2.094(6)
	BF	0.565	0.456	1.51(33)	1.91	3.89	2.18(1)		
0.030	OF	0.804	0.611	2.81(29)		4.06	2.19(1)	2.182(6)	2.192(4)
	BF	0.504	0.364	2.01(26)		7.30	2.19(1)		

Another contribution represents the extra kinetic energy due to the bending of the real part of the wave function close to the core. Finally there is a contribution due to the change of the expectation value of the Hamiltonian due to local rearrangement of the atoms close to the core. In Fig. 1 we plot also the contribution $v(r)$ of V_Ω to $\varepsilon_v(r)$. In the case of the OF phase, $\varepsilon_v(r)$ is significantly larger of $v(r)$ so that a substantial contribution to the vortex core energy is due to the bending kinetic energy. It is interesting to notice that $\varepsilon_v(r)$ is much closer to $v(r)$ in the case of the BF phase. Actually at freezing density and at $\rho = 0.03$ Å^{-3}, within the statistical uncertainty, $\varepsilon_v(r)$ coincides with $v(r)$; i.e., BF is so efficient that it essentially cancels the bending energy. At the two lowest densities of our computations there is some remaining contribution from the bending energy. We conjecture that this might be due to the choice of the BF phase Eq. (6) that is more accurate at large density and less so at lower density.

Classically the vortex energy (11) is simply proportional to the density if the vortex core parameter λ is density independent. We confirm the earlier finding [44] of the SWF computation that the energy of a quantum vortex in superfluid ^{4}He at short distance has very weak dependence on density. As reported in Table II $\varepsilon_v(r)$ at $r = 6$ Å within the statistical errors of our computation are the same at freezing and at equilibrium density.

Within the mean field GP equation the quantum vortex energy deviates from the hydrodynamic value (11) at short distance because the local density $\rho(r)$ is a function of r. From the numerical solution of the GP equation, accurate Padé approximants for the local density have been obtained [56,57]. Using the approximant [3/3] in Ref. [57]

$$f_{\rm GP}^2(r) = \frac{\rho(r)}{\rho} = \frac{0.3396r^2 + 0.0501r^4 + 0.0026r^6}{1 + 0.3976r^2 + 0.0527r^4 + 0.0026r^6}, \tag{12}$$

we have obtained the integrated vortex energy per unit length as

$$\varepsilon_v^{\rm GP}(r) = \pi \int_0^r \varrho d\varrho \left\{ [f'_{\rm GP}(\varrho)]^2 + \frac{f_{\rm GP}^2(\varrho)}{\varrho^2} + \frac{1}{2}\left[1 - f_{\rm GP}^2(\varrho)\right]^2 \right\}, \tag{13}$$

where the standard GP reduced units are used. In order to restore dimensional units for Eqs. (12) and (13), only a single parameter is required, i.e., the coherence (or healing) length ξ. Unfortunately, for strongly correlated systems as liquid ^{4}He, there is no unique definition for ξ. The standard procedure is to choose ξ such as the sound velocity provided by GP equation is equal to the observed one [58]. This leads to $\xi = 0.47$ Å at the equilibrium density and $\xi = 0.31$ Å at the freezing one. The authors of Ref. [17] proposed another recipe by requiring the GP core parameter (discussed below), which is about 1.5ξ, to be equal to the experimental value [59], resulting in $\xi = 0.87$ Å at the equilibrium density [60].

In Fig. 2 the SPIGS vortex energy $\varepsilon_v(r)$ is compared to the GP results for two choices for ξ as well as with the SWF variational results [44]. There is an overall good agreement

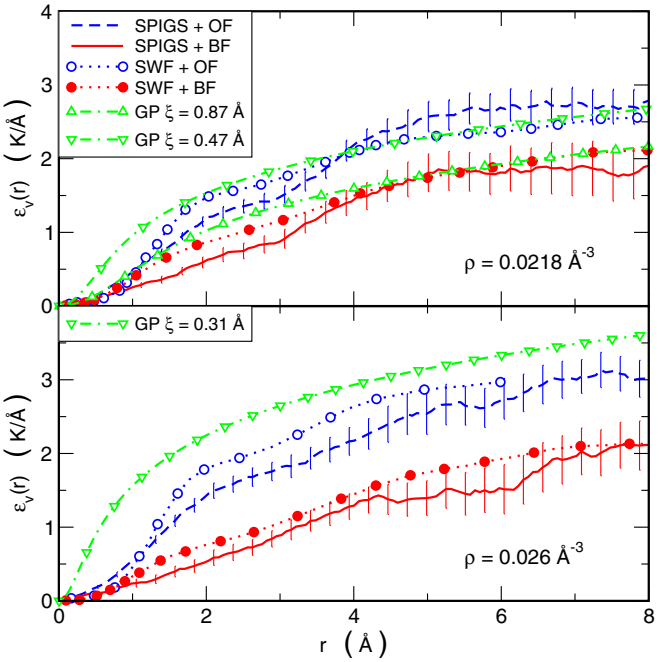

FIG. 2. (Color online) Comparison of integrated energy of a single vortex line per unit length, $\varepsilon_v(r)$, at equilibrium (upper panel) and freezing (lower panel) densities obtained with different methods.

between the SWF results and the present fixed phase SPIGS ones. This is an additional evidence of the excellent quality of SWF in representing superfluid ^{4}He. With respect to GP ones, one can say that it gives a reasonable representation of the vortex energy, but its quality very much depends on the value of the ill-determined parameter ξ. At equilibrium density the small value 0.47 Å gives $\varepsilon_v^{\rm GP}(r)$ in good agreement with the exact SPIGS result for the OF phase. What is surprising is that the GP result for $\xi = 0.87$ Å is rather close to the SPIGS result for BF phase. At the freezing density, the agreement of QMC data with GP predictions is poor when ξ is obtained in the standard way via the speed of sound.

Here a comment is in order. With SWF the total energy E_v of the vortex state and the energy E_0 of the ground state are each rigorously upper bounds to the exact values for the chosen model of the He-He interatomic potential, though no such bound is present for the vortex "excitation" energy $E_v - E_0$. On the other hand, in the fixed phase SPIGS computation both E_v and $E_v - E_0$ are upper bounds to the exact values because the SPIGS E_0 is exact within the statistical uncertainty. Finally, no bound is present for the vortex energy given by the GP equation.

In Fig. 3 we show the radial density profiles $\rho(r)$ obtained with the OF and BF phases. In qualitative agreement with the pioneering work by Chester *et al.* [10], $\rho(r)$ has a depression on the vortex axis and reaches the bulk density value in an oscillating way. $\rho(r)$ for the OF phase vanishes on the vortex core. At all studied densities $\rho(r)$ computed for the BF phase provides a partially filled core in qualitative agreement with the SWF results. As might be expected, the filling of the vortex core increases at large densities. By comparing the BF and OF density oscillations around the vortex core one can notice that such oscillations are significantly stronger for the OF phase and shifted to larger distance compared to the BF. These oscillations can be well fitted with a damped oscillating function [19,20]. Starting from $r \simeq 3$ Å we have fitted our density profiles $\rho(r)/\rho$ with the following functional form:

$$f(r) = f_0 + \frac{A}{\sqrt{r}} \cos(k_0 r + \phi) e^{-r/r_1} \tag{14}$$

with f_0, A, k_0, and r_1 fitting parameters. The damping parameter r_1 is reported in Table II. At all densities, the oscillations are more strongly damped when backflow is present. It is clear that backflow has the role of reducing the perturbation effect of the vortex and this explains the reduced core energy with respect to the OF phase.

As already pointed out, the core parameter is not rarely misled with the core radius, but we stress again that the core parameter λ is not a measure of the core extension; rather it is a suitable value to be inserted in the hydrodynamic description Eq. (11) to obtain the large distance behavior of the vortex energy. To obtain a measure of the vortex core extension is quite easy, even if not completely unequivocal, within the GP approach since the density profile $\rho(r)$ is a smoothly increasing function of r. The core radius is often taken equal to the radial distance where $\rho(r)/\rho = 1/2$ [17]. More difficult is to define it when $\rho(r)$ is an oscillating function of r as the ones shown in Fig. 3. As a possible choice we take $d_{\rm WHM}$ that we define as the position at which $\rho(r)$ is equal to the average of $\rho(r)$ at the first maximum and the value at the origin $r = 0$. The values of $d_{\rm WHM}$ are given in Table II. Such a core radius for the BF phase is significantly smaller of that for the OF phase and

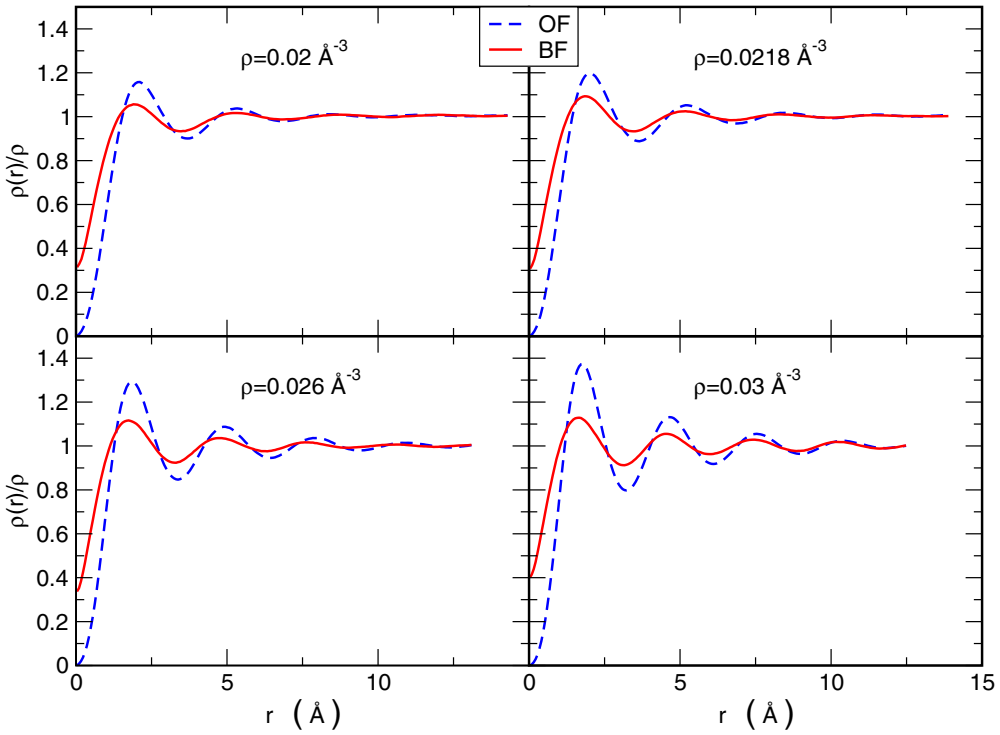

FIG. 3. (Color online) Radial density profiles, $\rho(r)/\rho$, for a single vortex line at different densities in liquid phase. Dashed line: Onsager-Feynman phase. Solid line: Backflow phase.

it shrinks for increasing density. We can obtain another way to measure the core radius in the following way. We might expect that at large distance from the core $\rho(r) = \rho$, so that $f_0 = 1$ in Eq. (14). We find that this is not so. The best fit of the computed $\rho(r)/\rho$ with Eq. (14) always gives f_0 slightly above 1; it is as if the average density far from the vortex core were $f_0\rho$. We can understand this as a result of the combined effect of operating with a fixed number of particles, of finite size of the simulation box, and of the expulsion of some particle from the vortex core. In fact, in our simulations, the particles removed from the core accumulate in the region far from the vortex line, increasing the average density. We define $R_{\rm cyl}$ as the radius of an impenetrable hard cylinder, coaxial with the vortex axis and completely void of particles, that inserted in the same simulation box gives rise to a density increase equal to $f_0\rho$. Thus $R_{\rm cyl}$ is also a measure of how many particles are expelled from the core of the vortex. The obtained values of $R_{\rm cyl}$ are given in Table II. $R_{\rm cyl}$ is of the same order of $d_{\rm WHM}$ and it has a similar dependence on the phase of the wf and on density.

The fixed phase SPIGS density profile at the equilibrium density is compared in Fig. 4 to the results of other theories. In the upper panel the results for the OF phase are shown. One can notice that there is a good agreement of the SPIGS result with that of the variational SWF computation [44]. As already noticed, the GP $\rho(r)$ is a monotonically increasing function of r; no oscillations are present. What is commonly

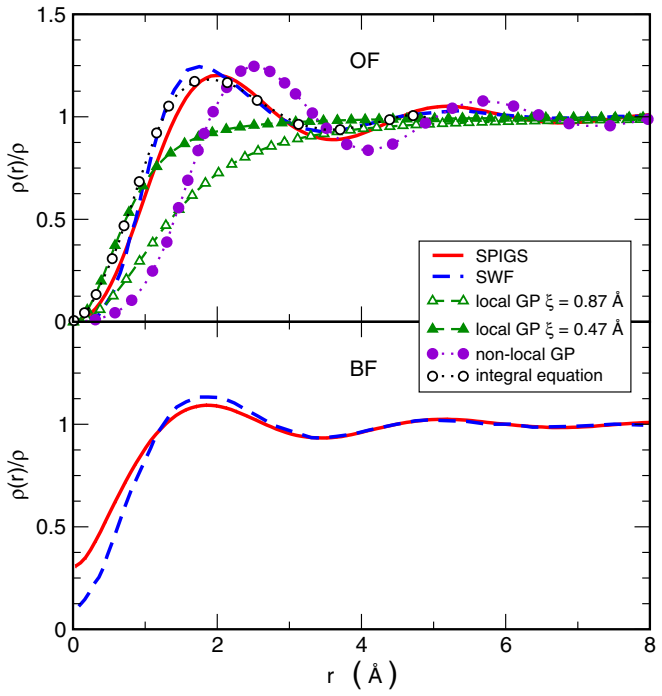

FIG. 4. (Color online) Comparison of normalized radial density profiles, $\rho(r)/\rho$, for a single straight vortex line at equilibrium density with Onsager-Feynman (upper panel) and backflow (lower panels) phases obtained with different methods. SPIGS results are from the present computation, SWF ones from Ref. [44]. Nonlocal GP result is from the model in Eq. (17) of Ref. [58] (with $\gamma = 1$, $\chi = 3.5$, and $\delta = 1$ in the notation of the original paper) and integral equation result is the one referred as B in Ref. [10].

called the GP equation is based, in addition to a mean field approximation, also on the assumption that the interatomic interaction $v(\vec{r}_1 - \vec{r}_2)$ is a contact one; i.e., $v(\vec{r}_1 - \vec{r}_2)$ is proportional to $\delta(\vec{r}_1 - \vec{r}_2)$. If one relaxes this assumption and takes a finite range $v(\vec{r}_1 - \vec{r}_2)$ one gets a nonlocal GP equation (also called nonlocal nonlinear Schrödinger equation) and $v(\vec{r}_1 - \vec{r}_2)$ has the role of a phenomenological effective interatomic potential between He atoms [4,61]. A further extension of GP has been studied in which a term proportional to a power higher than 4 of the single particle wf is included too [62]. The density profile around a straight vortex line as obtained with one of the most studied nonlocal GP models [58] is also reported in Fig. 4. It indeed gives an oscillating $\rho(r)$ with oscillations of amplitude comparable to those of the SPIGS computation, but the positions of the extrema are quite off the mark (remember that we are comparing theories with the same OF phase and that the SPIGS result is exact). Also the integral equation approach of Ref. [10] gives an oscillating $\rho(r)$ which is in overall good agreement with QMC results. In the lower panel of Fig. 4 the density profiles for two computations with backflow are shown, the present SPIGS and the SWF. The SPIGS result gives a larger population of the core and a somewhat smaller core size compared to the SWF result. Notice that the BF phase is not the same in these two computations; in the present computation the phase is explicit as given in Eq. (6) and it is variationally optimized, whereas in the SWF the phase is implicit because it derives from from a many-body integration over subsidiary variables.

In the context of density functional theory it has been proposed [19,20] that the oscillations of the local density around the vortex core could be related to the roton excitation. The range of densities considered in the present work corresponds to the range of densities recently studied [52] in the characterization of the excitation spectrum via the exact SPIGS method and GIFT [63], a novel powerful approach to extract dynamic structure factors from imaginary time density correlation functions. We have, therefore, the possibility to investigate such a relation on the basis of a fully microscopic approach. In order to estimate the wave vector associated with the density oscillation around the vortex core we have computed the Fourier transform, $\tilde{\rho}(q)$, of the radial density profile $\rho(r)/\rho - 1$. In computing $\tilde{\rho}(q)$, the SPIGS data have been extended with the function $f(r) - f_0$, from (14), beyond $L/2$. The obtained $\tilde{\rho}(q)$ are shown in Fig. 5. At each studied density a well defined peak is present in $\tilde{\rho}(q)$; its position, $q_{\rm max}$, indicates the wave vector which characterizes the oscillations in the radial density profile. The obtained $q_{\rm max}$ are reported in Table II together with the roton wave vectors [52], $q_{\rm rot}$, and the position of the main peak, q_χ, of the static density response function [64], $\chi(q)$, at the considered densities. We find that $q_{\rm max}$ is essentially the same for the OF and the BF phases, suggesting that it might be related to an intrinsic property of the bulk system. We find that even if they are very similar, $q_{\rm max}$ is always higher than the roton wave vector $q_{\rm rot}$; rather, we find a much better agreement with q_χ. This is not surprising since $\chi(q)$ provides the amplitudes of the density response of the system to a static perturbation, which is the case of a vortex within fixed phase approximation. Then q_χ corresponds to the preferred wave vector for a density modulation.

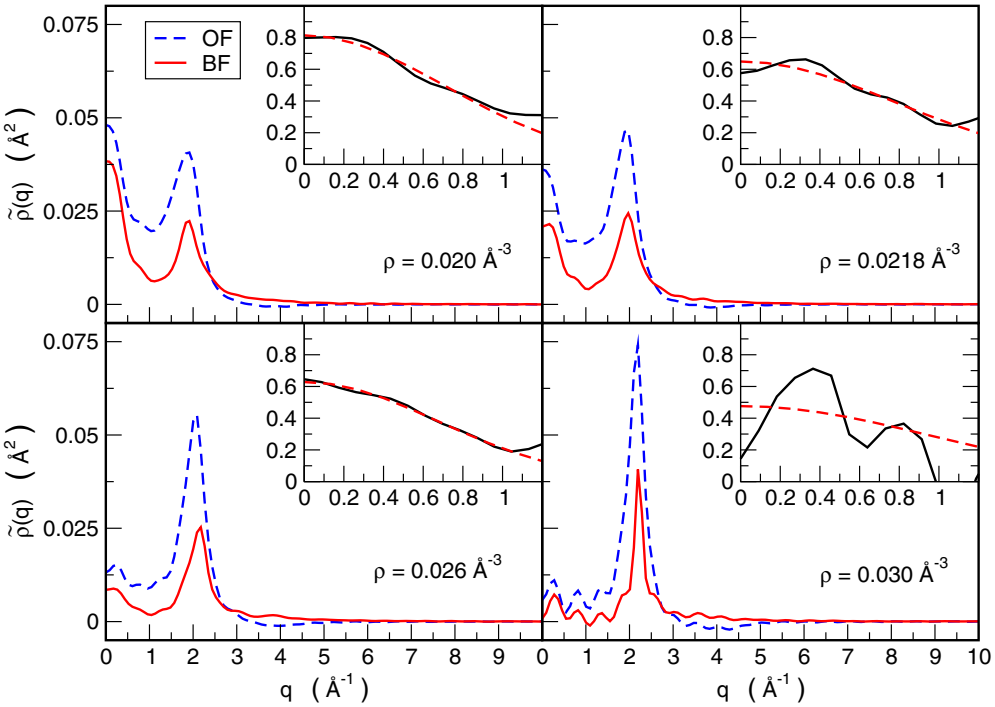

FIG. 5. (Color online) Fourier transform of the radial density profile, $\tilde{\rho}(q)$, for a single vortex line at different densities in liquid phase. Dashed line: Onsager-Feynman phase. Solid line: Backflow phase. Insets: Ratio between the Fourier transforms of the radial density profile with OF phase and with BF phase (solid line) and Gaussian fit in the $0 < q < 1$ Å^{-1} range (dashed line).

A vortex line has excited states in the form of Kelvin waves in which the vortex is no longer straight but its core moves in a helical way. One way of interpreting the delocalization of vorticity achieved with BF phase is that it is due to the zero point motion of such Kelvin waves. In fact, the localized vorticity given by the OF phase should spread out in a cylindrical region around the vortex axis as a consequence of such zero-point motion. Under such hypothesis the density profile $\rho_{\rm BF}(r)$ of the BF phase should be equal to the convolution of the density profile $\rho_{\rm OF}(r)$ of the OF phase and of the probability $P(r)$ that the vortex core has a transverse displacement equal to r. For harmonic oscillations $P(r)$ should be a Gaussian function. One can easily verify whether $\rho_{\rm BF}(r)$ indeed can be represented in this way. In fact, in Fourier space the convolution becomes a product, so the ratio of the Fourier transforms of $\rho_{\rm BF}(r)$ and $\rho_{\rm OF}(r)$ should be a Gaussian functions of the wave vector q. This ratio is plotted in the insets in Fig. 5 as well as the best fit by a Gaussian function over the range 0–1 Å^{-1}. It is clear that indeed the ratio $\tilde{\rho}_{\rm BF}(q)/\tilde{\rho}_{\rm OF}(q)$ is to a good approximation a Gaussian and this gives support to the notion that backflow for a vortex is a way to represent the zero point motion of Kelvin waves. The optimal fitting values for the variance of the Gaussian are 0.712 ± 0.016 Å at 0.020 Å^{-3}, 0.777 ± 0.044 Å at 0.0218 Å^{-3}, 0.676 ± 0.010 Å at 0.026 Å^{-3}, and 0.963 ± 0.016 Å at 0.030 Å^{-3}. A significant deviation of $\tilde{\rho}_{\rm BF}(q)/\tilde{\rho}_{\rm OF}(q)$ from a Gaussian is present only at the highest density $\rho = 0.030$ Å^{-3} in the metastable fluid phase. We do not know whether this is a genuine effect or whether it is a consequence of size effects that are more pronounced at higher density due to the slow decay of the density oscillations.

IV. LARGE VORTEX RING IN SUPERFLUID ^{4}He

Vortex ring excitations are particularly important for superfluid ^{4}He since experimental data [59] on mobility of ions trapped in the core of a vortex ring have given information on such excitations [55,59]. A full description of a vortex ring requires a more complex functional form for the phase, but for a large vortex ring, when the radius R is much larger than the core size, the energy is expected to be accurately approximated by the sum of the kinetic energy of an incompressible flow outside a toroidal region centered at the circle of radius R and with a radius b, and of the energy of the core inside this region [10]. This latter energy can be approximated by $2\pi R\varepsilon_v(b)$, where $\varepsilon_v(b)$ is the energy per unit length of a straight vortex line up to a distance b [10,25]. Here b represents the distance at which the inner quantum flow field is joined to the external hydrodynamic one and should not be confused with the core size or the healing length [25]. For the outer region the energy is the one of a classical vortex ring of radius R and a hollow core of size b:

$$E(R,b) = \frac{1}{2}\kappa^2 m\rho R\left[\ln\frac{8R}{b} - 2\right], \qquad (15)$$

where the circulation has been set to its quantum value $\kappa = h/m$. Then, within such an approximation, the excitation energy of a large vortex ring reads

$$E_{\rm ring}(R) = \frac{h^2}{2m}\rho R\left[\ln\frac{8R}{b} - 2 + \frac{4\pi m}{h^2\rho}\varepsilon_v(b)\right]. \qquad (16)$$

The experimental results of Rayfield and Reif [59] have been interpreted [55] in terms of an energy of a hollow-core

vortex ring of radius R, written in the form

$$E_{\rm ring}(R) = \frac{h^2}{2m}\rho R \ln\frac{8R}{\Lambda}. \quad (17)$$

Our approximated theoretical expression (16) can be recast in the form of (17) with the core parameter

$$\Lambda = be^{2-\frac{4\pi m}{h^2\rho}\varepsilon_v(b)}. \quad (18)$$

Our values of the parameter Λ are reported in Table I together with the values obtained by the fit over the experimental data [55]. In order to account for statistical uncertainty we have averaged Eq. (18) over the range $4 < b < 8$ Å where the computed energy per unit length is quite close to the hydrodynamic one (11). If the dependence of $\varepsilon_v(b)$ on b is well represented by Eq. (11), the energy of the ring (16) turns out to be independent of the choice of b [25], and the parameter Λ is equal to $e^2\lambda$. Our results excellently fulfill such a relation, with deviation smaller than 4%, confirming that, for large radial distances, the energy per unit length of a vortex line is given with great accuracy by the classical hydrodynamic functional form (11).

We stress again that the parameters λ in Eq. (11) and Λ in (17) do not represent the GP coherence length or the vortex core radius. Failure to recognize this can lead to an incorrect interpretation of experimental data. For instance, the interpretation of the experimental data in terms of classical hydrodynamics [55] led to a core parameter 0.81 Å and 1.04 Å, respectively, at equilibrium and at freezing density. This expansion of the core parameter with the density has been addressed as the test bed for any successful theory of the core structure, and a vortex model that fulfills this requirement has actually been developed [55]. However, if we consider the core parameter as a measure of the core extension we will be in the counterintuitive situation of a vortex that expands by increasing the density. This striking feature is due to a misleading interpretation of the hydrodynamic model (11). In fact, as shown in Table I, our theory with the BF phase gives at both equilibrium and freezing density results in rather good agreement with the experimental value of Λ, i.e., an expanding core parameter; but the actual core size, as measured by the density profile (parameters $d_{\rm WHM}$ and $R_{\rm cyl}$ in Table II), decreases by about 15% on going from equilibrium to freezing density. Moreover the vortex rings investigated in the experiments [55,59] have a radius in the decade 10^3–10^4 Å and it might be assumed that for such large vortices a full classical description should be adequate. In order to see that this is not correct consider the terms in square parentheses in Eq. (16). The factor $\frac{h^2\rho}{4\pi m}$ is 0.83 K/Å at equilibrium density and using $\varepsilon_v(b)$ for $b = 6$ Å from Table II we find that the third term in square parentheses in (16) is equal to 2.12. This term is equal to 1.51 when we perform a similar computation at freezing density. Thus if one does not take into account the variation with density of the quantum energy one gets an incorrect description of the vortex.

V. A MODEL FOR A VORTEX LINE IN SOLID ^{4}He

Given the recent interest on supersolidity and on the possible presence of vortex-like excitations in solid ^{4}He [31,33–36], we have extended our study also to the solid phase. Exact quantum Monte Carlo computation at finite [37,38] and zero temperature [40] have shown that an ideal perfect ^{4}He crystal (the so called commensurate solid) has no BEC and is not superfluid. Without the presence of BEC the standard order parameter cannot be defined and the form (3) or (6) for the phase of a quantum vortex has little justification because such a state should rapidly decay into other excitations. On the other hand it is known that almost any deviation from the ideal perfect state does induce BEC in solid ^{4}He [65–68]. The idea was to check the possibility that an ideal perfect ^{4}He crystal could correspond to a marginally stable quantum system [40] in which rotation would be a strong enough perturbation to induce a "dynamical" Bose-Einstein condensation and quantum vortices at the same time. In this case the OF and BF variational ansatz on the phase of the many-body wf could be justified for an order parameter defined at least locally [69]. Since the BF corrections have a larger effect on the core filling as the density is increased in the liquid phase, one could expect that BF should be even more relevant in the solid phase.

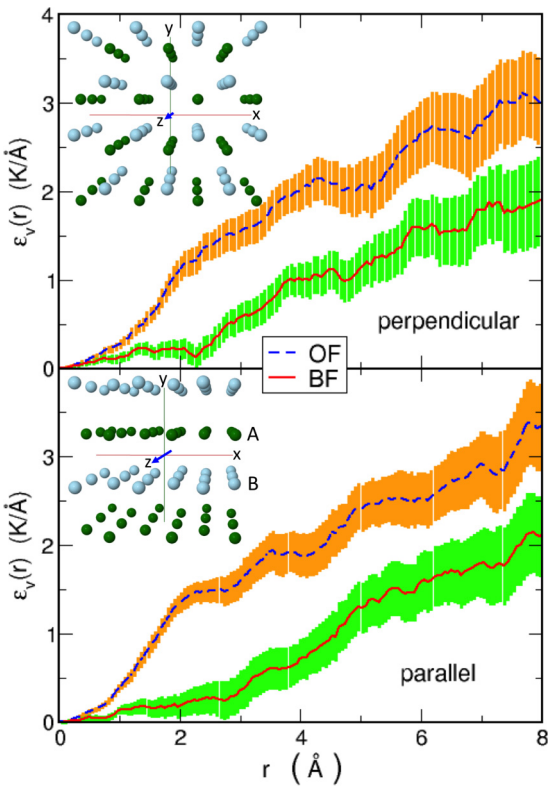

FIG. 6. (Color online) Integrated energy of a vortex line per unit length, $\varepsilon_v(r)$, at $\rho = 0.0293$ Å^{-3} in a hcp solid as function of the distance from the vortex core, for two different orientation of the vortex axis (which coincides with the z axis): perpendicular to the basal planes (upper panel) and parallel to the basal planes (lower panel) as shown in the insets where the vortex axis points toward the reader along the z axis. Atoms belonging to different basal planes in the hcp structure (A and B) have been represented with different colors. Dotted line: Onsager-Feynman phase. Solid line: Backflow phase. The shadings represent the statistical uncertainties of the results.

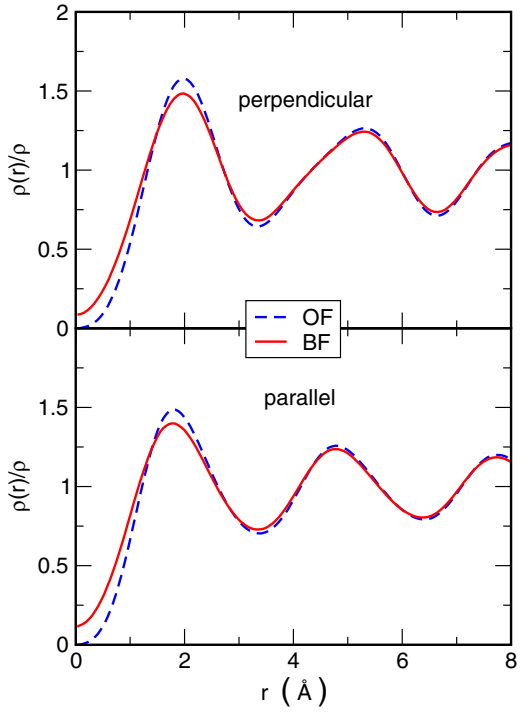

FIG. 7. (Color online) Normalized radial density profiles, $\rho(r)/\rho$, at $\rho = 0.0293$ Å^{-3} in a hcp solid as functions of the distance from the vortex core, for two different orientation of the vortex axis: perpendicular to the basal planes (upper panel) and parallel to the basal planes (lower panel). Dotted line: Onsager-Feynman phase. Solid line: Backflow phase.

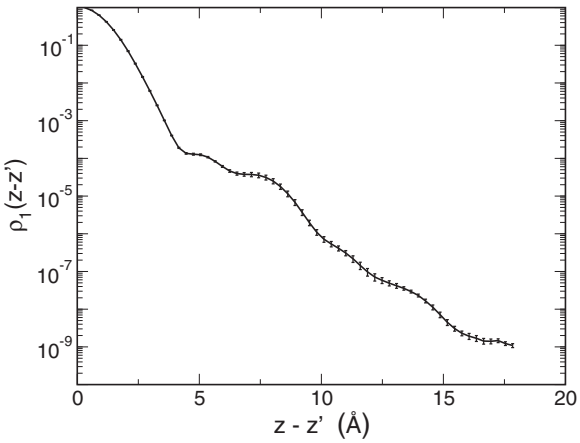

FIG. 8. One-body density matrix computed in a perfect hcp ^{4}He crystal at $\rho = 0.0293$ Å^{-3} along the direction parallel to the axis of the centrifugal flow field of the OF phase. The case shown here corresponds to an axis perpendicular to the basal planes of the hcp crystal.

We have thus performed fixed phase SPIGS computation for the OF (3) and the BF (6) phase also in bulk solid ^{4}He. In Fig. 6 we report the integrated energy per unit length $\varepsilon_v(r)$ and in Fig. 7 the radial density profile $\rho(r)/\rho$ as a function of the core distance r for the solution of Eq. (1) in an ideal perfect hcp ^{4}He crystal at $\rho = 0.0293$ Å^{-3}, just above the melting density. We have considered two possible orientations for the vortex axis: perpendicular to the basal planes (i.e., along the c axis) and parallel to the basal planes. As in the liquid phase, the BF phase provides an energy gain of about 1 K with respect to the OF one, but the most striking result is that the core is partially filled even in the solid phase when the BF phase is considered. The filling of the core is however smaller than that found in the liquid. Within the statistical uncertainty the obtained $\varepsilon_v(r)$ are the same for the two considered orientations of the vortex axis both with the OF and with the BF phase.

An interesting piece of information that we can derive from our computation is the deformation of the crystalline lattice and the location of the vortex axis with respect to the crystalline lattice sites. In fact, in a SPIGS computation the equilibrium positions of the atoms are generated as a spontaneous broken symmetry and the crystal is free to translate. We find that in the simulation, whatever is the starting configuration of the atoms with respect to the vortex axis the system evolves into a state in which the vortex axis is an interstitial line, in the sense that this straight line lies as far as possible from the lattice sites as shown in the insets in Fig. 6. A similar result was already noticed in two dimensional ^{4}He crystals [30]. In addition we find that the centrifugal barrier induces only a very small distortion of the crystal lattice, again in agreement with the result in 2D [30]. The vortex core filling is greater in the case where the axis of the centrifugal flow field is parallel to the basal planes; we have found, in fact, that in this case the solid is free to slide with respect to the axis and this gives rise also to a less structured density profile around core axis.

We have also computed the one-body density matrix $\rho_1(\vec{r},\vec{r}')$ in the system along the axis of the centrifugal flow field. We find that for both phases $\rho_1(\vec{r},\vec{r}')$ decays exponentially with increasing $|\vec{r}-\vec{r}'|$ as in the ideal perfect crystal. As an example, in Fig. 8 we show the result obtained for the one-body density matrix in the presence of a centrifugal flow field related to the OF phase with the axis perpendicular to the basal planes of a hcp ^{4}He crystal. A very similar result is obtained with the BF phase. We conclude that both the OF and the BF variational ansatz are not able to induce any off-diagonal long–range order in the crystal. This means that there is no condensate fraction induced by rotation and that the state corresponding to the solution of Eq. (1) is not a stable quantum state in an ideal perfect ^{4}He crystal. It should be noticed that it has been argued [70] that in solid ^{4}He vortices can appear also in the presence of a strongly fluctuating order parameter such that no phase coherence is present. Also in this case, the assumed forms (3) and (6) of the phase have little justification, so we cannot investigate this possibility with the present computation.

VI. CONCLUSIONS

We have performed a microscopic characterization of a single straight vortex line in three dimensional ^{4}He systems. By using unbiased quantum Monte Carlo methods at zero temperature and the fixed phase approximation, we have obtained an exact estimation of the local energy and the local

density profile around the vortex core once the Feynman-Onsager model or a phase with backflow correlations is assumed. The present results give a much stronger theoretical basis to some of the earlier findings obtained by the variational SWF method [25,47], such as the large lowering of the vortex core energy due to BF correlations, the weak dependence of the vortex core energy on density, or the significant oscillations of the density profile close to the core. In fact our results represent rigorous upper bounds of the exact excitation energy of a vortex. For the OF phase it is not possible to do better than our result because we solve exactly the quantum problem for the real part of the wf. With backflow our results depend on the specific choice of the BF phase so it could be improved. In any case our results allow us to conclude that it is not possible to get a correct quantitative estimation of the vortex core energy without taking into account backflow correlations. In fact the vortex excitation energy integrated up to a radial distance of order 2–4 Å is reduced by about a factor of 2 with respect to the value for the OF phase so any better BF phase would reduce that energy even more. The present results for a straight vortex line have important implications for vortex rings of radius much larger than the core radius and on interpretation of experimental data. It is customary to represent the energy and the translational velocity of the ring in term of formulae derived from hydrodynamics with the core parameter determined by the experimental data. We show that the energy of a vortex ring can indeed be represented with the hydrodynamic formula but the length parameter contained in it is not a measure of the size of the core but, as already shown in Ref. [44], it contains information on the core energy and this requires the quantum theory. Our results for the energy of the ring as function of its radius are in agreement with experiments both at equilibrium density and at freezing, at the same time the core radius shrinks for increasing density and the core parameter Λ expands. We remark that an increasing value of Λ with pressure, as obtained when the experimental data are interpreted by using the hydrodynamic description, is not a signature of an expanded vortex core.

Backflow not only reduces the excitation energy but also gives smaller oscillation of the density profile compared to the OF case and the density is finite even on the core axis. Analysis of the density profile with and without backflow shows that the first can be represented by a convolution of the second with a Gaussian function. This is suggestive that BF is a way to represent the effect of the zero point motion of Kelvin waves and from the width of the Gaussian we estimate a mean square oscillation of about 0.7 Å. This suggestion is worthy of further study. In Fourier space the density profile has a strong peak at a wave vector that at all densities is very close to the wave vector at which the static density response function has a maximum. This wave vector is somewhat larger than the one at the minimum of the roton dispersion curve so that our microscopic computations partially modify previous suggestions [19,20] based on phenomenological theories. The fact that the Fourier spectrum of the density profile is sharply peaked in q in the region of rotons with positive group velocity (so called R^+ rotons) gives a hint that in a vortex reconnection event there might be emission of rotons [18] in preference of phonons as obtained on the basis of GP equation [17]. Study of vortex reconnections with QMC methods to verify this prediction seems presently out of reach of microscopic simulation. It might be feasible to extend the GP study of reconnection to one of the nonlocal GP equations. For instance the model by Berloff and Roberts [58] is attractive because it gives a realistic description of the energetics of the roton excitations as well as a reasonable density profile around the vortex core as shown in Fig. 4. Should roton emission in a vortex reconnection depend more on the modulation of the density profile of the vortex than on the delocalized vorticity, it will be interesting to study the vortex reconnection with such an equation because it should give evidence for roton generation in a vortex reconnection. It has been also suggested in the literature [71] that around the vortex axis there might be a condensation of rotons. We do not find a way to prove or disprove such hypothesis on the basis of the present microscopic theory.

We have studied the vortex excitation also in metastable states below equilibrium density and above freezing. We do not find evidence of any anomaly for the studied densities; the vortex properties have a smooth density dependence within the statistics of our simulations.

A number of other properties of a vortex can be calculated with our simulation method. One is the computation of the flow field and of vorticity in the core region. This will allow one to compute the translational velocity of a large vortex ring with BF phase in a way similar to what was done in Ref. [10] for the OF model. Another interesting question is what happens to the Bose-Einstein condensate fraction n_0 in the core. It has been suggested [71] that in the core the fluid is normal even at $T = 0$ K. The only microscopic computation of the condensate for a vortex in superfluid ^{4}He is based on the integral equation method [10] and the result was an increasing condensate fraction n_0/ρ in the core but both n_0 and the local density were vanishing at the vortex axis because that computation was based on the OF phase. With BF phase the core is partially filled and it will be very interesting to compute n_0 with the present method. We leave such computations for future work. A further challenging development is the direct microscopic simulation of a small vortex ring.

We have investigated in crystalline solid ^{4}He a state with the same forms of the vortex phase as in the liquid phase. We find that the vortex core goes into interstitial positions and that there is a rather weak lattice distortion. At the same time we find that the system has no off-diagonal long-range order like in the perfect solid; i.e., the perturbation introduced by the phase is not able to induce a condensate. Therefore the studied excited state should not be a good representation of an elementary excitation of the solid. The topic of a microscopic model of the proposed vortex excitation in crystalline ^{4}He in the presence of a strongly fluctuating local order parameter [31] remains to be explored.

ACKNOWLEDGMENTS

We acknowledge the CINECA and the Regione Lombardia award, under the LISA initiative, for the availability of high-performance computing resources and support. One of us (L.R.) wants to thank Dipartimento di Fisica, Università degli Studi di Milano, for some support to his research activity.

[1] L. Onsager, Nuovo Cimento **6**, 279 (1949).
[2] R. P. Feynman, *Progress in Low Temperature Physics I*, edited by C. J. Gorter (North-Holland, Amsterdam, 1956).
[3] L. P. Pitaevskii, Zh. Eksp. Teor. Fiz. **40**, 646 (1961) [Sov. Phys. JETP **13**, 451 (1961)].
[4] E. P. Gross, Nuovo Cimento **20**, 454 (1961).
[5] P. G. Saffman, *Vortex Dynamics* (Cambridge University Press, Cambridge, 1992).
[6] A. L. Fetter, Rev. Mod. Phys. **81**, 647 (2009).
[7] M. Tsubota, M. Kobayashi, and H. Takeuch, Phys. Rep. **522**, 191 (2013).
[8] S. I. Davis, P. C. Hendry, and P. V. E. McClintock, Physica B **280**, 43 (2000).
[9] M. Tsubota, S. Ogawa, and Y. Hattori, J. Low Temp. Phys. **121**, 435 (2000).
[10] G. V. Chester, R. Metz, and L. Reatto, Phys. Rev. **175**, 275 (1968).
[11] R. P. Feynman and M. Cohen, Phys. Rev. **102**, 1189 (1956).
[12] D. E. Galli, E. Cecchetti, and L. Reatto, Phys. Rev. Lett. **77**, 5401 (1996).
[13] R. Rota, F. Tramonto, D. E. Galli, and S. Giorgini, Phys. Rev. B **88**, 214505 (2013).
[14] M. Rossi and L. Salasnich, Phys. Rev. A **88**, 053617 (2013).
[15] E. Fonda, D. P. Meichlea, N. T. Ouellette, S. Hormozf, and D. P. Lathrop, Proc. Natl. Acad. Sci. USA **111**, 4707 (2014).
[16] M. Leadbeater, T. Winiecki, D. C. Samuels, C. F. Barenghi, and C. S. Adams, Phys. Rev. Lett. **86**, 1410 (2001).
[17] S. Zuccher, M. Caliari, A. W. Baggaley, and C. F. Barenghi, Phys. Fluids **24**, 125108 (2012).
[18] S. Ogawa, M. Tsubota, and Y. Hattori, J. Phys. Soc. Jpn. **71**, 813 (2002).
[19] F. Dalfovo, Phys. Rev. B **46**, 5482 (1992).
[20] S. Villerot, B. Castaing, and L. Chevillard, J. Low Temp. Phys. **169**, 1 (2012).
[21] G. P. Bewley, D. P. Lathrop, and K. R. Sreenivasan, Nature (London) **441**, 588 (2006).
[22] G. P. Bewley, M. S. Paoletti, K. R. Sreenivasan, and D. P. Lathrop, Proc. Natl. Acad. Sci. USA **105**, 13707 (2008).
[23] D. E. Zmeev, F. Pakpour, P. M. Walmsley, A. I. Golov, W. Guo, D. N. McKinsey, G. G. Ihas, P. V. E. McClintock, S. N. Fisher, and W. F. Vinen, Phys. Rev. Lett. **110**, 175303 (2013).
[24] S. A. Vitiello, L. Reatto, G. V. Chester, and M. H. Kalos, Physica (Amsterdam) **194**, 699 (1994).
[25] S. A. Vitiello, L. Reatto, G. V. Chester, and M. H. Kalos, Phys. Rev. B **54**, 1205 (1996).
[26] G. Ortiz and D. M. Ceperley, Phys. Rev. Lett. **75**, 4642 (1995).
[27] R. P. Feynman, Phys. Rev. **94**, 262 (1954).
[28] D. E. Galli and L. Reatto, Mol. Phys. **101**, 1697 (2003).
[29] D. E. Galli and L. Reatto, J. Low Temp. Phys. **134**, 121 (2004).
[30] M. Rossi, D. E. Galli, P. Salvestrini, and L. Reatto, J. Phys.: Conf. Ser. **400**, 012063 (2012).
[31] P. W. Anderson, Nat. Phys. **3**, 160 (2007).
[32] M. H. W. Chan, R. B. Hallock, and L. Reatto, J. Low Temp. Phys. **172**, 317 (2013); **173**, 354(E) (2013).
[33] A. Penzev, Y. Yasuta, and M. Kubota, J. Low Temp. Phys. **148**, 677 (2007).
[34] A. Penzev, Y. Yasuta, and M. Kubota, Phys. Rev. Lett. **101**, 065301 (2008).
[35] H. Choi, D. Takahashi, K. Kono, and E. Kim, Science **330**, 1512 (2010).
[36] H. Choi, D. Takahashi, W. Choi, K. Kono, and E. Kim, Phys. Rev. Lett. **108**, 105302 (2012).
[37] M. Boninsegni, N. V. Prokofev, and B. V. Svistunov, Phys. Rev. Lett. **96**, 105301 (2006).
[38] B. K. Clark and D. M. Ceperley, Phys. Rev. Lett. **96**, 105302 (2006).
[39] E. Vitali, M. Rossi, F. Tramonto, D. E. Galli, and L. Reatto, Phys. Rev. B **77**, 180505 (2008).
[40] D. E. Galli and L. Reatto, J. Phys. Soc. Jpn. **77**, 111010 (2008).
[41] E. Sola, J. Casulleras, and J. Boronat, Phys. Rev. B **76**, 052507 (2007).
[42] S. Giorgini, J. Boronat, and J. Casulleras, Phys. Rev. Lett. **77**, 2754 (1996).
[43] E. W. Draeger, Ph.D. thesis, University of Illinois at Urbana Champaign, 2001.
[44] M. Sadd, G. V. Chester, and L. Reatto, Phys. Rev. Lett. **79**, 2490 (1997).
[45] J. K. Nilsen, J. Mur-Petit, M. Guilleumas, M. Hjorth-Jensen, and A. Polls, Phys. Rev. A **71**, 053610 (2005).
[46] The authors of Ref. [42] found a hollow core even with BF correction because their trial wave function maintains a divergence of the velocity field at the vortex core.
[47] M. Sadd, G. V. Chester, and F. Pederiva, Phys. Rev. Lett. **83**, 5310 (1999).
[48] S. A. Vitiello, K. Runge, and M. H. Kalos, Phys. Rev. Lett. **60**, 1970 (1988).
[49] T. MacFarland, S. A. Vitiello, L. Reatto, G. V. Chester, and M. H. Kalos, Phys. Rev. B **50**, 13577 (1994).
[50] M. Rossi, M. Nava, D. E. Galli, and L. Reatto, J. Chem. Phys. **131**, 154108 (2009).
[51] R. A. Aziz, V. P. S. Nain, J. S. Carley, W. L. Taylor, and G. T. McConville, J. Chem. Phys. **70**, 4330 (1979).
[52] M. Rossi, E. Vitali, L. Reatto, and D. E. Galli, Phys. Rev. B **85**, 014525 (2012).
[53] R. J. Donnelly, *Quantized Vortices in Helium II* (Cambridge University Press, Cambridge, 1981).
[54] A. L. Fetter in *The Physics of Liquid and Solid Helium*, Part 1, edited by K. H. Bennemann and J. B. Ketterson (Wiley, New York, 1976), Chap. 3.
[55] W. I. Glaberson and R. J. Donnely, in *Progress in Low Temperature Physics*, edited by D. Brewer (North-Holland, Amsterdam, 1986), Vol. IX.
[56] N. G. Berloff, J. Phys. A: Math. Gen. **37**, 1617 (2004).
[57] C. Rorai, K. R. Sreenivasan, and M. E. Fisher, Phys. Rev. B **88**, 134522 (2013).
[58] N. G. Berloff and P. H. Roberts, J. Phys. A: Math. Gen. **32**, 5611 (1999).
[59] G. W. Rayfield and F. Reif, Phys. Rev. **136**, A1194 (1964).
[60] The authors of Ref. [17] used as an experimental value for the core parameter a the one given in Ref. [59]. This value had been obtained from the experimental results for energy and velocity of vortex rings via a solid core model keeping the quantum of circulation κ as a fitting parameter. The authors of Ref. [55] provide a different set of values by using a hollow core model and with κ set to its theoretical value. We shall compare our results with this second set of data, since even in our computation κ is fixed to its theoretical value.
[61] Y. Pomeau and S. Rica, Phys. Rev. Lett. **71**, 247 (1993).

[62] J. Dupont-Roc, M. Himbert, N. Pavlov, and J. Treiner, J. Low Temp. Phys. **81**, 31 (1992).
[63] E. Vitali, M. Rossi, L. Reatto, and D. E. Galli, Phys. Rev. B **82**, 174510 (2010).
[64] T. Minoguchi and D. E. Galli, J. Low Temp. Phys. **162**, 160 (2011).
[65] D. E. Galli and L. Reatto, Phys. Rev. Lett. **96**, 165301 (2006).
[66] L. Pollet, M. Boninsegni, A. B. Kuklov, N. V. Prokofev, B. V. Svistunov and M. Troyer, Phys. Rev. Lett. **98**, 135301 (2007).
[67] M. Boninsegni, A. B. Kuklov, L. Pollet, N. V. Prokofev, B. V. Svistunov and M. Troyer, Phys. Rev. Lett. **99**, 035301 (2007).
[68] M. Rossi, E. Vitali, D. E. Galli, and L. Reatto, J. Phys.: Condens. Matter **22**, 145401 (2010).
[69] K. Yamamoto, Y. Shibayama, and K. Shirahama, Phys. Rev. Lett. **100**, 195301 (2008).
[70] P. W. Anderson, J. Low Temp. Phys. **169**, 124 (2012).
[71] W. J. Glaberson, D. M. Strayer, and R. J. Donnelly, Phys. Rev. Lett. **21**, 1740 (1968).